Resonant cavity-enhanced quantum-dot infrared photodetectors with sub-wavelength grating mirror

Chi-Cheng Wang and Sheng-Di Lin

Citation: Journal of Applied Physics **113**, 213108 (2013); doi: 10.1063/1.4809574
View online: http://dx.doi.org/10.1063/1.4809574
View Table of Contents: http://scitation.aip.org/content/aip/journal/jap/113/21?ver=pdfcov
Published by the AIP Publishing

Resonant cavity-enhanced quantum-dot infrared photodetectors with sub-wavelength grating mirror

Chi-Cheng Wang and Sheng-Di Lin[a)]
Department of Electronics Engineering, National Chiao Tung University, 1001 University Road, Hsinchu 300, Taiwan

(Received 18 February 2013; accepted 21 May 2013; published online 5 June 2013)

We propose and simulate a device structure of resonant cavity-enhanced quantum-dot infrared photodetector (RCE-QDIP). The RCE-QDIP consists of a conventional n-i-n QDIP sandwiched by a bottom GaAs/Al_2O_3 distributed Bragg reflector and a top mirror of Ge/SiO_2 sub-wavelength grating. Aiming for detecting mid-infrared at 8 μm, the total thickness of the device is only $\sim$7.7 μm. According to our simulation, the external quantum efficiencies of RCE-QDIP could be as high as 59%-78% with the enhancement factors of 7–30, compared with a conventional QDIP. The proposed RCE-QDIP is highly feasible as the various fabrication parameters are considered.
 [http://dx.doi.org/10.1063/1.4809574]

I. INTRODUCTION

Quantum-dot infrared photodetectors (QDIP) have been attracting attentions for more than a decade due to their potential applications on mid-infrared detection.[1–4] The 3D confinement and the nearly defect-free quality of self-assembled quantum dots (QDs) make them suitable to detect normally incident light at definite wavelengths. By engineering the nanostructures around QDs, the detection wavelength can be selected and the device performance have been improved significantly recently.[5–7] However, comparing with other types of infrared photodetectors (PDs), such as quantum well infrared photodetectors (QWIP) or HgCdTe-based photodiodes, QDIP has very low quantum efficiency mainly because of the small absorption cross section and discrete density states of QDs.[1,4] To improve the quantum efficiency, a straight way is to increase the areal density and/or the number layers of QDs. This method can enhance the responsivity of the device but it is limited by the accumulation of strain arising from the lattice mismatch between the dot and matrix materials.[2] An elegant solution to this is placing a QDIP into a resonant cavity to maximize the absorption of light. Resonant cavity-enhanced PDs (RCE-PDs) have been developed for long time and its flexibility makes nearly 100% quantum efficiency achievable even for those materials with extremely small absorption coefficients.[8–11] In the past years, works on using resonant cavity or field enhancement to improve the quantum efficiency of QDIP have been reported and the enhancement factors of 12 in experiment and of 17 in theory have been demonstrated.[12–16] Different from the QWIPs with resonant cavity design,[17,18] the intrinsic quantum efficiency of QDIPs is much lower so a high-reflectivity mirror is needed. To fabricate a mirror in the mid-infrared regime (3–5 or 8–12 μm) requires a very thick either distributed Bragg reflector (DBR) or cavity which makes the sample growth and/or device fabrication much more difficult. To overcome the problem with DBR, one can use the two alternative layers having large difference in refractive index to reduce the number of layers needed for high reflectivity.[12,13] Instead of typical AlAs/GaAs DBRs, Attaluri *et al*. used 1.5-periods AlO_x (oxidized from AlAs) and GaAs DBR as the bottom mirror and GaAs/air interface as the front mirror, and a quantum efficiency of $\sim$10% was obtained at about 9.5 μm.[12] In Asano's work, two-pair GaAs/air-gap back mirror achieved a 12-fold enhancement of the detectivity at $\sim$4.3 μm.[13] A further improvement can be made if a high reflectivity front mirror is introduced. Kang proposed a metal grating as the front mirror for dual wavelength resonance and predicted a 13-times enhancement at 9.9 μm.[16] However, the structure included a very thin substrate with a precise thickness for resonance, which is not very practical for device fabrication.

On the other hand, the emerging of sub-wavelength dielectric grating attracts much attention owing to its novel optical properties and flexibility in integrating with other devices.[19–26] With a single layer serving as a grating and also a waveguide, the sub-wavelength grating exhibits wide-band high-reflectivity based on the guided-mode resonance (GMR) effect. Benefiting from its much thinner thickness and flexibility during device processing, the GMR reflector has been implemented in many photonic devices instead of conventional DBR mirror.[19–21] Previously, we have demonstrated both theoretically and experimentally that a high-reflectivity (>95%) GMR mirror at 8 μm can be realized by 2-μm-thick Ge/SiO_x on GaAs substrate.[27] In this paper, we propose and analyze a RCE-QDIP consisting of a bottom DBR mirror of 1.5-periods Al_2O_3/GaAs, a top GMR mirror of Ge/SiO_2, and a cavity of a conventional n-i-n QDIP in between. As we shall present, this RCE-QDIP with total thickness of about 7.7 μm is promising to solve the problem of low quantum efficiency in conventional QDIPs in a flexible way. More importantly, as we shall discuss, our design is easy and feasible for sample growth and device fabrication so one can foresee the realization of QDIP with high quantum efficiency in coming years.

[a)]E-mail: sdlin@mail.nctu.edu.tw

II. DEVICE DESIGN AND SIMULATION PARAMETERS

A. Design concept

In the aspect of optical consideration, a RCE-PD consists of three parts, a bottom mirror, a cavity with absorption layer, and a top mirror. To maximize the detection efficiency, the reflectivity of bottom mirror has to be as high as possible, which is typically achieved with a DBR reflector. Regarding to the cavity layer, once the detection wavelength has been assigned, the thickness and materials can be decided accordingly. The reflectivity of the top mirror, however, has to be optimized based on the absorption of the cavity layer.[8–10] A general rule is that smaller absorption needs higher reflectivity to obtain the optimized quantum efficiency. With a proper design, a RCE-PD can achieve nearly 100% quantum efficiency. Here, we place a conventional n-i-n QDIP into a resonant cavity, as shown in Fig. 1. The cavity is formed with two mirrors, a top GMR mirror of Ge subwavelength grating laid on a SiO_x layer and a bottom DBR mirror of GaAs/AlO_x. In the following, we shall explain the design concept for individual parts in detail.

Let us start with the top GMR mirror first. GMR is a coupling effect between the grating diffraction and the guided mode.[22–25] In a single-layer GMR grating, the grating itself also serves as a waveguide layer. That is, as the diffracted rays couple into the guided mode of grating, a resonant condition can be met to make the reflected light interference constructively so nearly 100% reflectivity could be achieved.[24,27] Ge is chosen as the grating material for two reasons: its refractive index at 8 μm is as high as 4.0 and it is transparent in the mid-IR regime (>2 μm). The underneath SiO_x layer is needed to provide the guiding effect in the Ge grating/waveguide because of its low refractive index. However, as mentioned above, to maximize the absorption with the resonant cavity, the reflectivity of the front GMR mirror has be varied with the absorption of the QD layers. An ideal GMR mirror for RCE-QDIP, therefore, is a broad band reflector with appropriate reflectivity in the QDs' absorption regime. Regarding to the bottom DBR mirror, to minimize the film thickness for epitaxy, we choose a 1.5-periods AlO_x/GaAs DBR reflector. The AlO_x can be formed by wet-oxidizing $Al_{0.98}Ga_{0.02}As$ or AlAs/GaAs digital alloys at high temperature (~400–450 °C).[28]

B. Simulation parameters

To verify our design concept, numerical simulations based on the method of rigorous coupled-wave analysis[26] are performed with the commercial software, DIFFRACTMOD3.1, produced by RSoft Design Group. By inputting the structure parameters of thickness and refractive index of each material, the reflectivity/absorption/transmission spectra and steady-state electric field distribution can be calculated accordingly. The structure and parameters used in our simulation are detailed in Fig. 2. The RCE-QDIP includes three parts, GMR mirror, resonant cavity, and DBR mirror. The top GMR reflector is a strong refractive-index-modulation 2D grating consisting of Ge and air. The hexagonal-lattice grating as shown in Fig. 2(b) has a period a of 5 μm and a hole radius r of 1.65 μm, which gives an r/a ratio of 0.33. The low-refractive-index SiO_2 layer underneath is necessary for wave guiding in the Ge grating. The GMR mirror itself has a thickness of 1630 nm and a reflectivity of about 0.79 at ~8 μm. Under the top mirror, the resonant cavity is basically a conventional n-i-n QDIP with specific thickness aiming for 8-μm resonance. The QDs are embedded in an $In_{0.15}Ga_{0.85}As$ quantum well (dots-in-a-well, DWELL) with inserted $Al_{0.3}Ga_{0.7}As$ for enhancing confinement.[7] Ten layers of such QDs are placed with 50-nm-thick GaAs spacers in between. The total thickness of the cavity layer is $T_c = 2.514$ μm. Finally, the bottom DBR mirror is formed with a 599-nm-thick GaAs sandwiched with two Al_2O_3 layers with thickness of 1493 nm, which is designed as the quarter wavelength of 8 μm. The simulated reflectivity of the 1.5-period DBR mirror is ~90%. Higher reflectivity is even better for enhancing the absorption but a thicker total thickness is undesirable for device fabrication. In our design, the total thickness for III-V materials growth using either molecular beam epitaxy (MBE) or metal-organic chemical vapor deposition (MOCVD) is about 6.1 μm provided that there is no volume shrinkage during the oxidation of AlAs into Al_2O_3.[28] The rectangular unit cell for simulation is shown in Fig. 2(b). The used refractive indices of GaAs (n-typed or undoped), Ge, and Al_2O_3 are 3.341, 4.0, and 1.34, respectively.[29] For SiO_x, we use the optical parameters provided by the library of the software.

Owing to the difficulty of simulating 3D QDs, instead, we used a 2D InAs film with a refractive index of 3.515.[29]

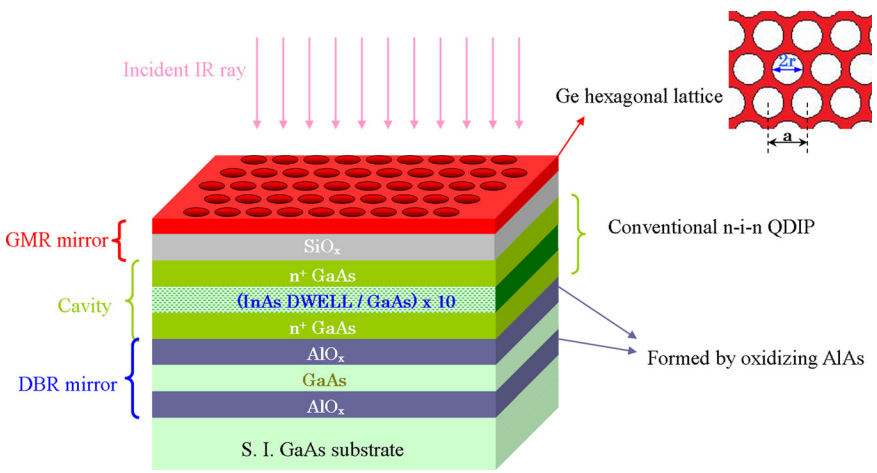

FIG. 1. Schematics of a RCE-QDIP with a top Ge/SiO_x GMR reflector, a bottom AlO_x/GaAs DBR mirror, and a cavity of conventional n-i-n QDIP. The upper-right figure shows the Ge hexagonal lattice with a period of a and a hole radius of r.

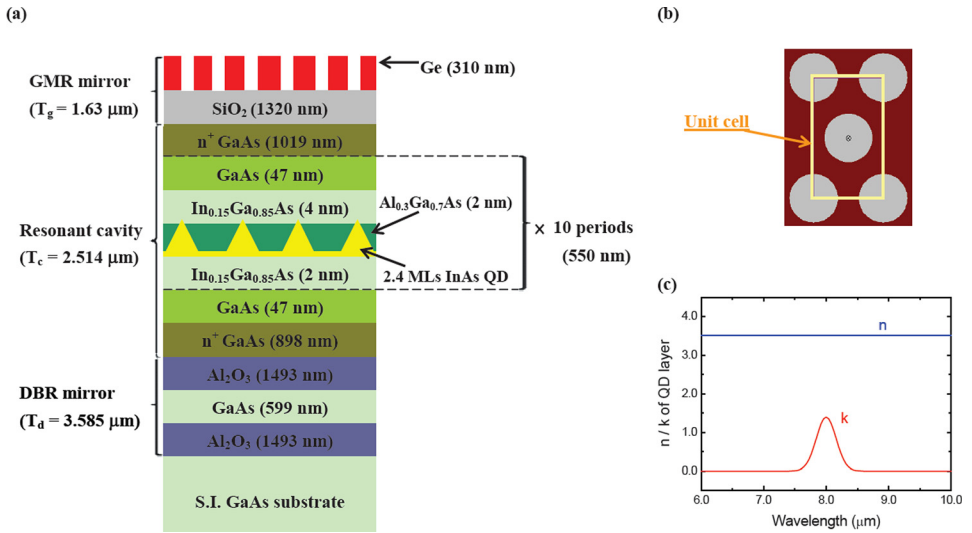

FIG. 2. Structure and parameters used in our simulation. (a) Materials and thickness of each layer. Note that the InAs QDs is replaced with a 2D InAs film in simulation; (b) defined unit cell; (c) refractive index n and extinction coefficient k of one QD's layer.

The absorption coefficient of QDs is difficult to assign because it varies among published reports and is very sensitive to layer structures and growth conditions. We extract the extinction coefficient k of one QD's layer from the measured quantum efficiency η by using the following equations:[30]

$$\eta = (1-R)(1-e^{-N\alpha t}), \tag{1}$$

$$k = \alpha\lambda/4\pi. \tag{2}$$

The R is the reflectivity of GaAs/air interface, N is the number of QDs' layers, t is the used InAs film thickness in simulation, and λ is the measured peak wavelength (8 μm). For the time being, we set $\eta = 3\%$, $R = 0.3$, $N = 10$, and $t = 2$ nm so the resultant α is 2.19 μm^{-1} and peak k is 1.394. The extinction coefficient spectra of QDs is modeled with a Gaussian function from 7.5 to 8.5 μm with a full-width at half-maximum (FWHM) of 0.37 μm, as illustrated in Fig. 2(c). Note that, because the absorption of QDs is highly uncertain, we shall discuss its effect on our RCE-QDIP device later.

III. RESULTS AND DISCUSSIONS

A. Absorption spectra and field distribution

The simulated absorption spectra of the RCE-QDIP are plotted in Fig. 3(a), together with the reflection and transmission spectra. A strong absorption with a peak value of ~0.592 is obtained at 8.0 μm. Compared with the original external quantum efficiency of 3%, an enhancement factor of 19.7 is expected, if the electrons generated by the absorption can be effectively collected. This enhancement factor is the highest one in the reported literatures. Note that the FWHM is 0.2 μm that is smaller than that of extinction coefficient (0.37 μm) because of the resonant effect. At the wavelength of 8 μm, the reflectivity is nearly zero (~0.016) but the transmission is quite high ~0.392. So an even stronger absorption could be achieved with a higher reflectivity of the DBR mirror. This can be done with one more pair of Al_2O_3/GaAs but the total film thickness has to be increased. In Fig. 3(b), we plot the electric field distribution for 8-μm infrared ray along the center axis of the hole on the Ge grating. The cavity length is approximately one λ and the anti-node locates approximately at the center. The positions of QDs' layers are also plotted in the same figure so we can see the good alignment of QDs' layers with the maximum of electric field. This good alignment results the strong absorption at 8 μm as shown in Fig. 3(a). Even for the top and bottom QDs' layers, the located electric field is still quite high, about 70% of the peak value. The spacer between QDs' layers could be narrower to place more QDs' layers into the regions of high electric field if the strain accumulation is not an issue. The

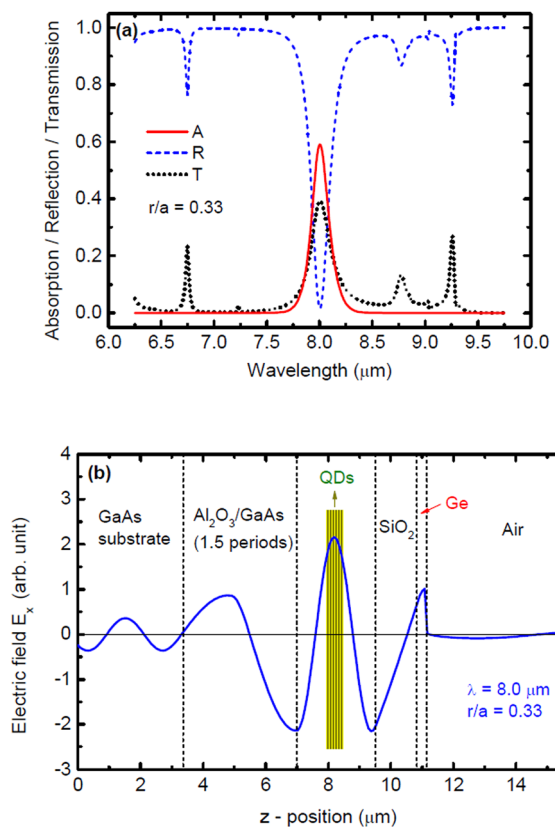

FIG. 3. (a) Simulated absorption, reflection, and transmission spectra; (b) electric field distribution along the axis of hole center in Fig. 2(b).

field intensity being very weak in air but being considerably strong in the GaAs substrate is consistent with the nearly zero reflection and the moderate transmission as shown in Fig. 3(a).

B. Considerations of processing parameters

To examine the feasibility of our design, we consider the possible processing error in device fabrication and sample growth here. Four possible errors are considered: (a) the hole radius of the Ge grating; (b) the thickness of Ge layer; (c) the thickness of SiO_2 layer; and (d) the thickness of the cavity layer (T_c). The first three errors arise from the processing imperfection and the last one could be because of the incorrect growth rate in MBE or MOCVD. The simulation results are plotted in Fig. 4. In Fig. 4(a), the devices with r/a ratios of 0.27 and 0.39 are compared with the ideal structure (the one in Fig. 2) with 0.33 r/a ratio. The peak wavelength and the maximum value of absorption are nearly unchanged. Note that the hole radius for r/a ratio of 0.27 (0.39) is 1.35 μm (1.95 μm) so the corresponding photo-lithography error is ± 0.3 μm. The thickness error of Ge and SiO_2 sourcing from the deposition equipments is set as $\pm 10\%$. As shown in Figs. 4(b) and 4(c), the problem caused by these errors can be disregarded. However, for the cavity layer, the thickness error is indeed a problem. In Fig. 4(d), we plot the cases of $\pm 5\%$ error in the thickness of cavity layer (T_c). A shorter cavity length ($T_c = 2.388$ μm) exhibits a blue shift in the resonant wavelength, as expected. Even worse, owing to the narrow absorption bandwidth of QDs, the maximum absorption decreases significantly. A similar situation occurs in the case of a longer cavity length. Therefore, the cavity length is the most sensitive fabrication parameter needed to be taken care of. Actually, this problem could be solved by growing a little bit thicker top n^+-GaAs layer (the one under SiO_2 layer). By etching the additional n^+-GaAs to a proper depth, one can align the cavity length with the absorption peak of grown QDs' layers.

We have also calculated the incident angle dependence of the device as it happens in many applications. In Fig. 5, for the ideal structure with r/a ratio of 0.33, the angle dependence of peak absorption/reflection/transmission is plotted. It is clear that the peak absorption is unaffected for the incident angle less than 10° but decreases to about 0.2 at 20° because of increased reflection of the grating.

C. Effect of intrinsic QDs' absorption and grating reflectivity

Among the all parameters used in this work, the most uncertain one is the extinction coefficient k that is deduced from the measured quantum efficiency η as mentioned above. It is possible to calculate the absorption coefficient directly from the shape and composition of QDs and the surrounding matrix materials but this approach is difficult and its results are usually not consistent with experiments. Deducing the absorption coefficient of QDs from the measured η is also not very accurate because not every absorption-generated electron can escape the QDs and be collected by the contact. To address this issue, we study the dependence of the device absorption on QDs' absorption coefficient by varying the extinction coefficient k. Besides, we have also examined four kinds of gratings with different reflectivity at 8 μm. The four gratings have the same r/a ratio of 0.33 but different thicknesses of Ge and SiO_2, as listed in the inset table of Fig. 6(a). Note that the GMR mirror C is the one already presented above. At 8 μm, the reflectivity of GMR mirrors A, B, C, and D are about 0.65, 0.75, 0.79, and 0.82, respectively, based on the simulation of the GMR

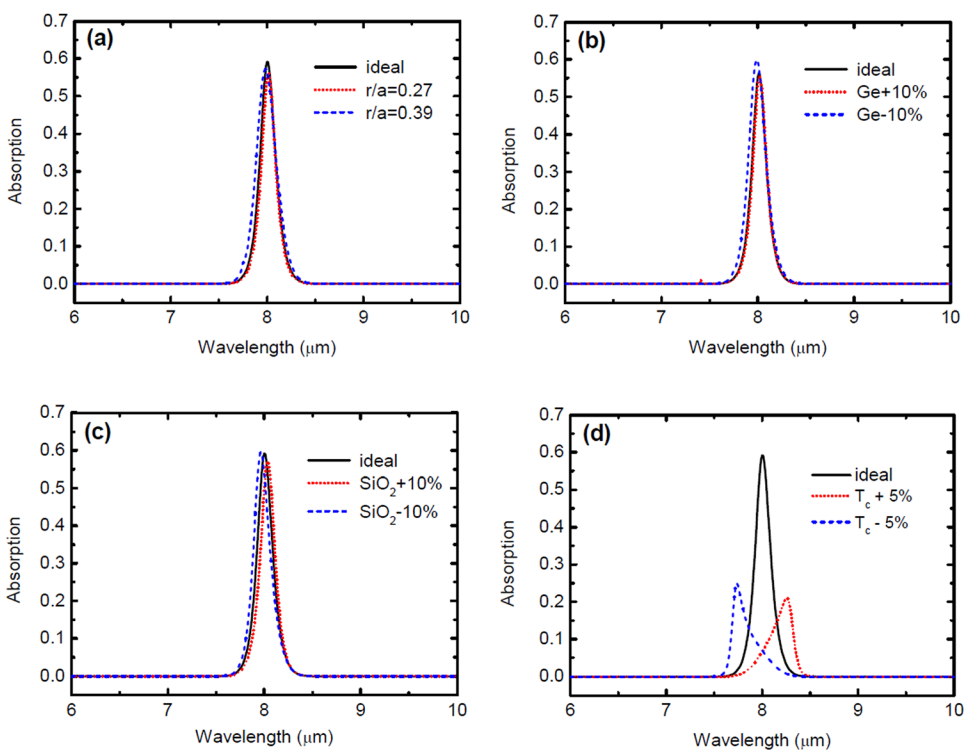

FIG. 4. Simulated absorption spectra of the RCE-QDIPs with fabrication errors: (a) r/a ratios of 0.27, 0.33, and 0.39; (b) Ge layer thickness of 279, 310, and 341 nm; (c) SiO_2 layer thickness of 1188, 1320, and 1452 nm; (c) cavity length T_c of 2.388, 2.514, and 2.640 μm.

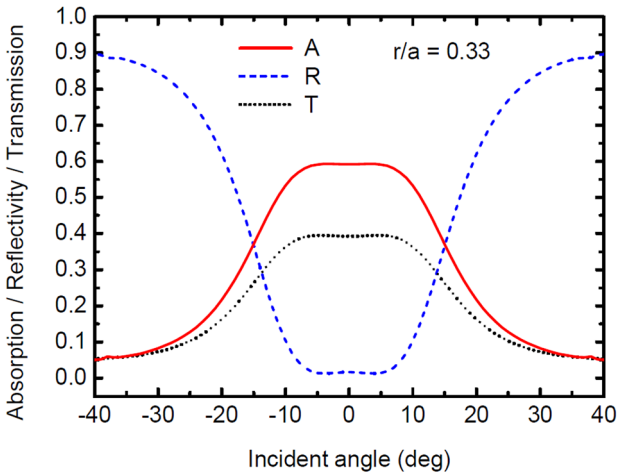

FIG. 5. Absorption/reflectivity/transmission of the RCE-QDIP against the incident angles of 8-μm infrared.

mirrors on GaAs substrate only. In the QD's absorption regime (7.5–8.5 μm), the reflectivity slightly decreases with increasing wavelength. With these four gratings, we simulate the device absorption against the original quantum efficiency, as shown in Fig. 6(b). The original quantum efficiency is used to calculate the corresponding extinction coefficient k by Eqs. (1) and (2). All other parameters are the same as those in Fig. 2 except that four GMR mirrors (A, B, C, and D) are employed for comparison.

First, let us see the curve C in Fig. 6(b), the absorption of RCE-QDIP with mirror C first increases rapidly with increasing original quantum efficiencies and falls gradually after reaching a peak value of 0.657. Similar trend is observed in other RCE-QDIPs. The maximum absorptions of those with mirrors A, B, and D are 0.784, 0.699, and 0.592, respectively. The maximum absorptions occur at different original quantum efficiencies because the device with a higher front mirror reflectivity has the absorption maximum at lower absorption coefficient, which is consistent with the analysis reported previously.[8–10] This reveals that, in order to achieve the highest absorption of RCE-QDIP, one could either design a better grating for the QDs with certain absorption coefficient or tune the absorption of QDs (for example, change the number of QDs' layers) for a given front GMR mirror. In addition, the detection linewidth at maximum absorption decreases with increasing grating reflectivity as expected. The detection linewidths are about 0.29, 0.22, 0.20, and 0.15 μm for the gratings A, B, C, and D, respectively. The simulation result of the QDIP without the top and bottom mirrors (that is, $T_g = T_d = 0$ in Fig. 2) is also plotted in Fig. 6(b) for comparison, which confirms that our simulation results are correct. By dividing the absorption of the RCE-QDIP with mirrors A, B, C, and D with that of QDIP without cavity, we can calculate the enhancement factors for the four devices at all original quantum efficiencies, as shown in Fig. 6(c). The enhancement factors decrease with the increasing original quantum efficiencies as expected.[8,9] At the original quantum efficiency of 1%, the RCE-QDIP with mirror D has the highest enhancement factor of 30.7. The enhancement factors of the four devices

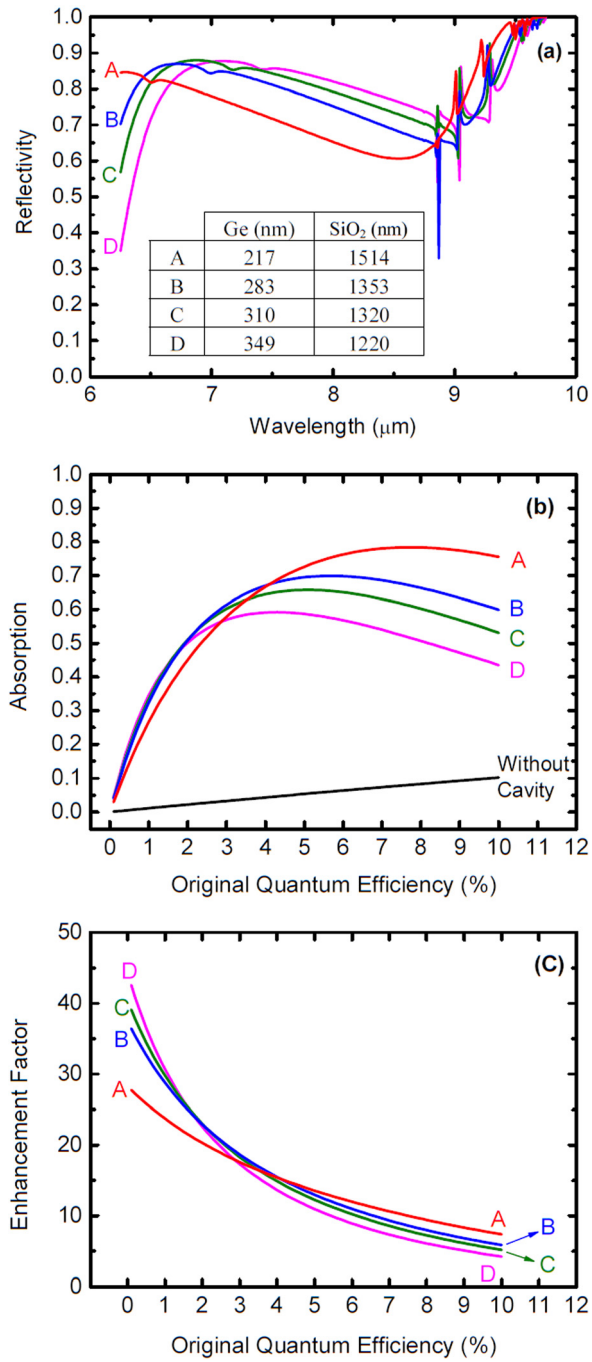

FIG. 6. (a) The reflectivity spectra of the four GMR mirrors with the thickness of Ge and SiO_2 listed in the inset; (b) simulated absorption of the four RCE-QDIPs with GMR mirrors A, B, C, and D against the original quantum efficiency; (c) the enhancement factors of absorption for the four devices.

are around 20 and quite close to each other at the original quantum efficiency of 3%. At the original quantum efficiency of 10%, the highest enhancement factor of 7.4 is obtained in the RCE-QDIP with mirror A. It is worth noting that the free carrier absorption of n^+-GaAs layers has not been taken into account in the simulation shown above. We did simulate the effect for $n^+ = 1 \times 10^{18}\,cm^{-3}$ based on the parameter given by Ref. 31 and found that its effect on device absorption negligible. To reduce the free carrier absorption further, one can use low doping concentration for

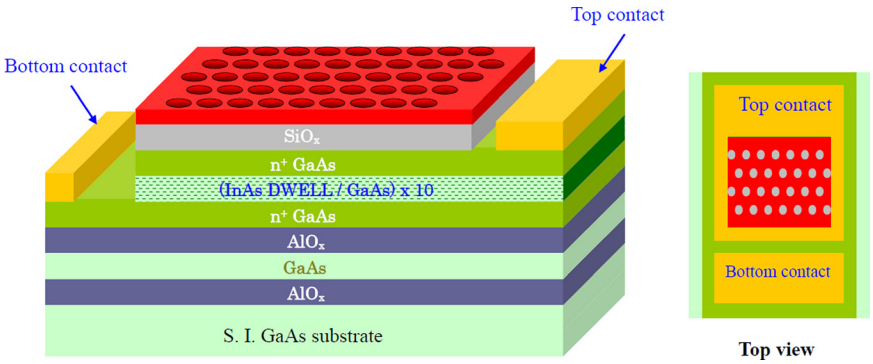

FIG. 7. Schematics for the processed device.

n-type GaAs layers as the device performance of QDIPs is usually not affected by its serial resistance. According to these results, we can conclude that our resonant cavity design is promising to boost the performance of a conventional QDIP by increasing its responsivity.

In Fig. 7, the fabricated device structure is sketched schematically. We suggest that the fabrication starts with the deep etching to expose the two AlAs layers on the front and back sides for subsequent wet oxidation process. The top and bottom contacts can be formed at the same time after an additional etching opening the bottom n^+-GaAs layer. The device top view is illustrated in Fig. 7 showing the suggested contact arrangement for single device. To make focal plane array with the RCE-QDIP would have a lower filling factor as the top contact takes away certain chip area.

IV. CONCLUSION

We presented the theoretical considerations of a RCE-QDIP using GMR effect as the top mirror and an Al_2O_3/GaAs DBR reflector as the bottom mirror. The proposed device structure can significantly enhance the infrared absorption in a conventional QDIP. The fabrication method has been presented although processing problems need to be solved before making a focal plane array of high fill factor with our design. By considering the issues on sample growth and device processing, the simulation confirms the feasibility of our devices so we expect the experimental demonstration of QDIPs with high quantum efficiency in the near future.

ACKNOWLEDGMENTS

This work was financially supported by the National Science Council and by the ATU Program of Ministry of Education in Taiwan. We thank Professor C. P. Lee and Professor Gray Lin for their helpful discussions. Preliminary works on GMR mirrors done by Mr. K. W. Lai are highly appreciated.

[1]A. Rogalski, J. Antoszewski, and L. Faraone, J. Appl. Phys. **105**, 091101 (2009).
[2]S. Chakrabarti, A. D. Stiff-Roberts, X. H. Su, P. Bhattacharya, G. Ariyawansa, and A. G. U. Perera, J. Phys. D: Appl. Phys. **38**, 2135 (2005).
[3]T. E. Vandervelde, M. C. Lenz, E. Varley, A. Barve, J. Shao, R. V. Shenoi, D. A. Ramirez, W. Yang, Y. D. Sharma, and S. Krishna, IEEE Sel. Top. Quantum Electron. **14**, 1150 (2008).
[4]P. Martyniuk and A. Rogalski, Prog. Quantum Electron. **32**, 89 (2008).
[5]S. Y. Wang, S. D. Lin, H. W. Wu, and C. P. Lee, Infrared Phys. Technol. **42**, 473 (2001).
[6]S. Krishna, J. Phys. D: Appl. Phys. **38**, 2142 (2005).
[7]H. S. Ling, S. Y. Wang, C. P. Lee, and M. C. Lo, Appl. Phys. Lett. **92**, 193506 (2008).
[8]K. Kishino, M. S. Unlu, J. I. Chyi, J. Reed, L. Arsenault, and H. Morkoc, "Resonant cavity-enhanced (RCE) photodetector," IEEE J. Quantum Electron. **27**, 2025 (1991).
[9]M. S. Unlu and S. Strite, J. Appl. Phys. **78**, 607 (1995).
[10]S. D. Lin and C. P. Lee, Semicond. Sci. Technol. **17**, 1261 (2002).
[11]J. P. Kim and A. M. Sarangan, Opt. Express **12**, 4829 (2004).
[12]R. S. Attaluri, J. Shao, K. T. Posani, S. J. Lee, J. S. Brown, A. Stintz, and S. Krishna, J. Vac. Sci. Technol. B **25**, 1186 (2007).
[13]T. Asano, C. Hu, Y. Zhang, M. Liu, J. C. Cambell, and A. Madhukar, IEEE J. Quantum Electron. **46**, 1484 (2010).
[14]R. V. Shenoi, J. Rosenberg, T. E. Vandervelde, O. J. Painter, and S. Krishna, IEEE J. Quantum Electron. **46**, 1051 (2010).
[15]C. C. Chang, Y. D. Sharma, Y. S. Kim, J. A. Bur, R. V. Shenoi, S. Krishna, D. Huang, and S. Y. Lin, Nano Lett. **10**, 1704 (2010).
[16]G. Kang, I. Vartiainen, B. Bai, and J. Turunen, Opt. Express **19**, 770 (2011).
[17]A. Shen, H. C. Liu, M. Gao, E. Dupont, M. Buchanan, J. Ehret, G. J. Brown, and F. Szmulowicz, Appl. Phys. Lett. **77**, 2400 (2000).
[18]Y. F. Lao, G. Ariyawansa, and A. G. Unil Perera, J. Appl. Phys. **110**, 043112 (2011).
[19]Y. Zhou, M. C. Y. Huang, C. Chase, V. Karagodsky, M. Moewe, B. Pesala, F. G. Sedgwick, and C. J. Chang-Hasnain, IEEE J. Sel. Top. Quantum Electron. **15**, 1485 (2009).
[20]K. W. Lai, S. D. Lin, Y. S. Lee, and Y. J. Fu, Opt. Express **20**, 3572 (2012).
[21]Y. S. Yang, Y. Q. Huang, X. M. Ren, X. A. Ye, X. F. Duan, H. Huang, and Q. Wang, Adv. Mater. Res. **93–94**, 43 (2010).
[22]S. S. Wang, R. Magnusson, J. S. Bagby, and M. G. Moharam, J. Opt. Soc. Am. A **7**, 1470 (1990).
[23]A. Sharon, D. Rosenblatt, and A. A. Friesem, J. Opt. Soc. Am. A **14**, 2985 (1997).
[24]C. F. R. Mateus, M. C. Y. Huang, Y. Deng, A. R. Neureuther, and C. J. Chang-Hasnain, IEEE Photon. Technol. Lett. **16**, 518 (2004).
[25]S. Peng and G. M. Morris, Opt. Lett. **21**, 549 (1996).
[26]M. G. Moharam and T. K. Gaylord, J. Opt. Soc. Am. **71**, 811 (1981).
[27]K. W. Lai, S. D. Lin, Z. L. Li, and C. C. Wang, "Long-wavelength mid-infrared reflectors using guided-mode resonance," Appl. Opt. (submitted).
[28]G. W. Pickrell, J. H. Epple, K. L. Chang, K. C. Hsieh, and K. Y. Cheng, Appl. Phys. Lett. **76**, 2544 (2000).
[29]*Handbook of Optical Constants of Solids*, edited by E. D. Patik (Elsevier, 1998).
[30]B. E. A. Saleh and M. C. Teich, *Fundamentals of Photonics*, 2nd ed. (Wiley, 2007), p. 172.
[31]K. Osamura and Y. Murakami, Jpn. J. Appl. Phys., Part 1 **11**, 365 (1972).